

A Group-Theoretic Analysis of Symmetric Target Scattering With Application to Landmine Detection

James M. Stiles, *Senior Member, IEEE*, Abhjit V. Apte, and Beng Beh

Abstract—Landmines are generally constructed such that they possess a high level of geometric symmetry and are then buried in a manner that preserves this symmetry. The scattered response of such a symmetric target will likewise exhibit the symmetry of the target, as well as the electromagnetic reciprocity exhibited by all scatterers. Group theory provides a mathematic tool for describing geometric symmetry, and it can likewise be used to describe the symmetries inherent in the bistatic scattering from mines. Specifically, group theory can be used to determine specific forms of the dyadic Green's function of symmetric scatterers, such that multiple scattering solutions can be determined from a knowledge of a single bistatic geometry. Likewise, group theory can be used both to determine and analyze degenerate cases, wherein specific bistatic responses can be identified as zero regardless of target size, shape, or material. These results suggest a method for classifying subsurface targets as either symmetric or asymmetric. From the group-theoretic analysis, scattering features can be constructed that are indicative of target symmetry, but invariant with respect to other target parameters such as size, shape, or material. These features provide a physically based, target-independent value to aid in mine detection and/or clutter rejection. To test the efficacy of this idea, an extensive collection of bistatic ground-penetrating radar (GPR) measurements was taken for both a symmetric and an asymmetric target. The two targets were easily discernable using symmetry features only, a result that suggests symmetry features can be effective in identifying subsurface targets.

Index Terms—Bistatic radar, ground-penetrating radar (GPR), group theory, landmines, symmetry.

I. INTRODUCTION

GROUND-PENETRATING radar (GPR) has long been considered as a sensor for detecting the presence of buried landmines [1], [2]. For obvious reasons, the required probability of detection for any demining sensor is typically extremely high, which unfortunately can lead to high false-alarm rates when subsurface clutter (e.g., rocks, shell casings) are present. As a result, a GPR system using simple energy detection is generally insufficient for mine detection; target discrimination is also required. A GPR sensor must, therefore, collect sufficient information such that a subsurface object can be detected and then correctly classified as either a mine or a clutter object.

Manuscript received August 6, 2001; revised January 14, 2002. This work was supported by the Office of the Secretary of Defense under Contract Number DAAG55-97-1-0014 "Multi-Disciplinary Research on Mine Detection and Neutralization Systems" and was managed by the U.S. Army Research Office.

J. M. Stiles is with the Radar Systems and Remote Sensing Laboratory, University of Kansas, Lawrence, KS 66044 USA.

A. V. Apte is with Sprint's Broadband Wireless Group.

B. Beh is with Winbond Electronic Corporation America, San Jose, CA USA.

Publisher Item Identifier 10.1109/TGRS.2002.802503.

A radar collects information about an object by observing a portion of its scattered response as a function of time/frequency, spatial position (e.g., bistatic scattering angle), and polarization. Therefore, a target can be correctly identified only if this scattered response is known *a priori* and is unique with respect to all other possible targets. Some investigators have used measured radar data of both mines and clutter to identify unique scattering responses [3], [4], whereas others have developed algorithms that rely on numeric electromagnetic formulations to compute the scattered responses of mines [5], [6]. These processors have proven to be very powerful and have significantly reduced the false-alarm rate associated with many GPR sensors.

A seemingly unavoidable problem faced by any target identification technique, however, is the vast diversity of mine target responses. Worldwide, hundreds of different mine models have been, or are currently being, produced. Additionally, the scattering responses from these mines are dependent on other factors such as soil dielectric and mine depth. Investigators have developed statistical processors to account for these parametric uncertainties [7], but the general problem of implementing a specific processor for each mine remains.

An argument can be made, however, that target *identification* is not explicitly required for demining. Rather, target *classification* is an acceptable objective. In other words, a sensor that either could accurately declare a target as a mine or as a benign clutter object would be sufficient; specifically identifying the type or model of the mine is not required. A classification sensor could, therefore, implement just a single processor, one that generically recognizes the scattering from any mine. Of course, a prerequisite for this approach is the existence of a detectable scattering response common to all mines, yet distinct from every clutter object. If such a response exists, a processor independent of mine type could be created. Given the wide variance of possible mine sizes, shapes, and materials, as well as variations in buried depth and the surrounding soil characteristics, such a common response might seem unlikely.

However, there is one physical feature that is not only common to most buried mines, but is generally not exhibited by clutter objects. Since mines are man-made, they typically exhibit structural symmetries that are not commonly found in natural objects, such as rocks. Furthermore, unlike other man-made clutter, buried mines are nominally oriented such that their symmetry is preserved with respect to the surface plane. The question then is in what manner, if any, does target symmetry manifest itself in electromagnetic scattering? Can target symmetry be recognized from GPR observations, and can a processor be constructed that can effectively classify targets as either symmetric or asymmetric?

This paper attempts to provide some answers to these questions. In Section II, the mathematical subject of group theory is briefly discussed, as well as its application to the analysis of geometric symmetry. In Section III, this group-theoretic approach is extended to describe bistatic observations of a symmetric target. It is shown that target symmetry results in spatial and polarization symmetry in the scattering response. A new group, referred to as the *bistatic group*, is defined to describe the symmetries of the electromagnetic scattering from symmetric targets. In Section IV, it is shown that the bistatic group can also be used to determine the general form of the dyadic Green's function of a symmetric object, regardless of its other physical parameters. Finally, in Section V, the results of Section IV are used to construct symmetry measures from bistatic measurements, measures that provide a numeric indication of the observed target symmetry. An experiment is then described wherein these symmetry measures were calculated from a large collection of bistatic measurements. It is then shown that these values provide an effective scattering feature for classifying a subsurface object as either symmetric or asymmetric.

II. TARGET SYMMETRY

Three-dimensional (3-D) objects often exhibit geometric symmetries with regard to rotation, reflection, and translation. These types of symmetries are visually intuitive and are evident in art and architecture throughout antiquity. During the 20th century, group theory [8], [9] was used to form a mathematical description of geometric symmetry, thus providing an analytic tool for solving physical problems where symmetry appears, most notably in the fields of physical chemistry and quantum mechanics [10]. In recent years, group theory has also been more frequently applied to problems in electrical engineering, including signal processing, and the analysis of symmetric networks, components, antennas, and scatterers [11]–[17, pp. 252–263].

A group \mathcal{G} of transformations is defined as a set of N operations g_n . This set must be closed: any two sequential operations must be equivalent to another element in the group (i.e., $g_i g_j = g_k$). Additionally, a group must include an identity operation e , as well as an inverse operation g_n^{-1} (such that $g_n g_n^{-1} = e$) for each element of the group. The operations of a group are associative, but may not be commutative. Operations represented by group element g_n can include geometric transformations, such as rotations, reflections, and combinations thereof. Groups consisting of these operations are referred to as point groups and are used to specify the geometric symmetry of an object. Mathematically, the symmetry exhibited by an object is defined as an invariance to all operations of a specific point group. In other words, if an object is congruent under every geometric transformation (i.e., element) of a given point group, then the object is said to possess the symmetry of that group. The order of a group is defined as the number of closed operations N that define the group, so that the symmetry of an object can be characterized by this order—the higher the order, the more symmetric the object.

For example, consider the object displayed in Fig. 1(a). We can reflect this object across the vertical plane defined by the

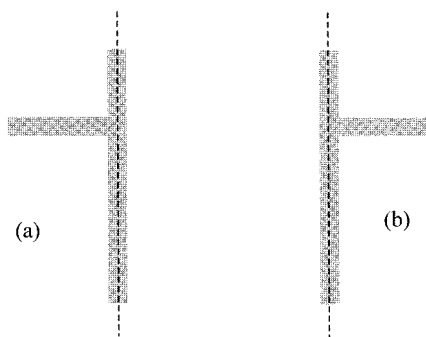


Fig. 1. Arbitrary object after operation by each element of group \mathcal{P} . Note the resulting objects have shapes that are not congruent.

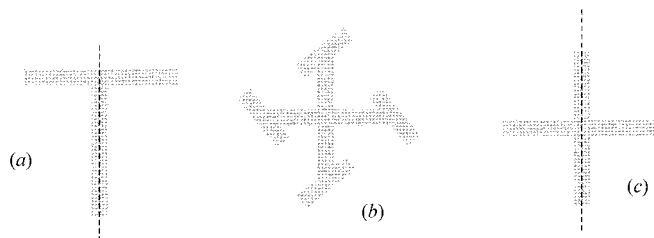


Fig. 2. Three objects [(a), (b), and (c)] that are congruent under all operations of group \mathcal{P} , X_4 , and X_{4a} , respectively.

dotted line, with the result depicted in Fig. 1(b). If a second reflection is performed, the object returns to its original state [see Fig. 1(a)]. Thus, a double reflection is equivalent to an identity operation: the object is not modified by the operation. Note this set of two operations is closed, i.e., any sequence of these operations is equivalent to one or the other of these operations. Additionally, each operation is also its own inverse. Thus, these two geometric operations—identity and reflection—define a point group of order two, denoted as \mathcal{R} .

The object in Fig. 1(a) is not congruent under all operations of \mathcal{R} , as the reflection operation modifies the original object shape. The object, therefore, does not possess the reflection symmetry defined by \mathcal{R} , nor, in fact, does it possess the symmetry of any nontrivial point group. Conversely, the object displayed in Fig. 2(a) is congruent under every operation of group \mathcal{R} ; reflecting the object across the vertical plane results in precisely the original shape. Since this object is congruent under every operation of group \mathcal{R} , it is described as possessing reflection (or bilateral) symmetry \mathcal{R} . Furthermore, the object of Fig. 2(b) exhibits rotational symmetry, as it is congruent under rotations of $\pi/2$. This object possesses \mathcal{C}_4 symmetry (using the Schoenflies notation [18]), where \mathcal{C}_4 denotes the cyclic point group of order 4. Finally, Fig. 2(c) displays an object that exhibits both reflection and rotational symmetry; it possesses \mathcal{C}_{4a} symmetry, where the subscript **a** denotes that the reflection plane includes the axis of rotational symmetry (it could alternatively be orthogonal to it). Accordingly, this third object is congruent under all eight operations of group \mathcal{C}_{4a} .

Square landmines typically possess \mathcal{C}_{4a} symmetry, whereas rectangular mines have \mathcal{C}_{2a} symmetry. Additionally, many landmines exhibit shapes that are (or nearly are) bodies of revo-

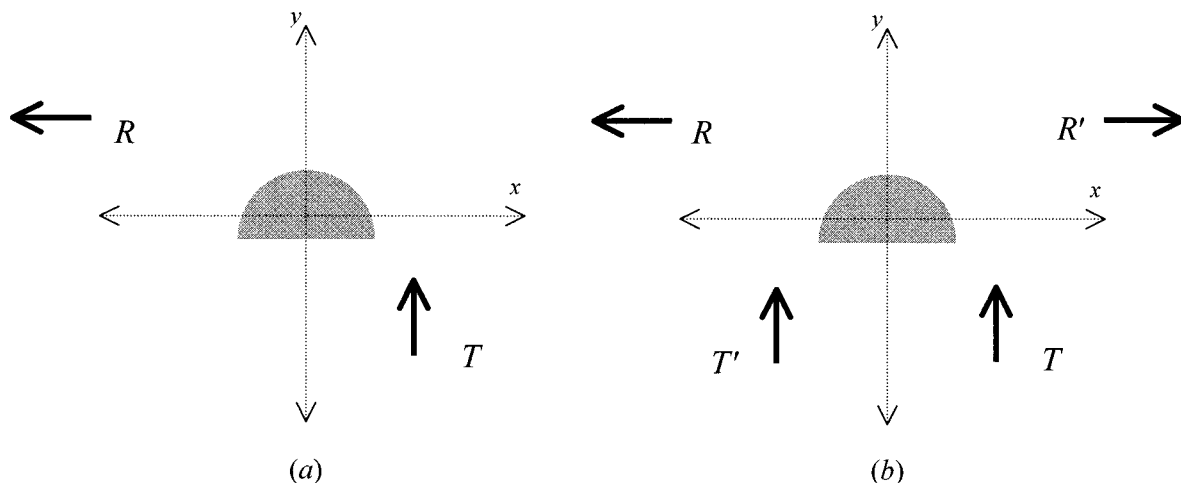


Fig. 3. (a) Bistatic measurement that is invariant with respect to group P operating on the target. This is equivalent to (b), where the operations of P are alternatively applied to the bistatic measurement. The two resulting bistatic measurements (primed and unprimed) must, therefore, be identical.

lution (BOR). These objects are said to possess $\mathcal{C}_{\infty a}$ (or \mathcal{O}_2) symmetry, as BORs are congruent under an infinite number of angular rotations. Additional point groups include the dihedral group, the rotation-reflection group, and the groups associated with regular polyhedra [19]. As the symmetries associated with these groups are not generally exhibited by landmines, they are not explicitly addressed in this paper.

III. BISTATIC GROUP

Consider a bistatic GPR observation, as demonstrated by Fig. 3(a). The two arrows define the position and orientation of a bistatic antenna pair (we assume Hertzian dipoles), located just above the soil, while the observed target is buried beneath the surface. This target is a half-sphere, oriented such that its flat side is parallel to the plane $y = 0$. Since this object exhibits bilateral symmetry across the plane $x = 0$, applying any geometric operation of group \mathcal{R} to the target will result in an identical object. As such, the bistatic measurement of this target after each operation will be identical: just like the target shape, the measurement is invariant with regards to operations of group \mathcal{R} . In contrast, consider the case where the geometric operations of the \mathcal{C}_4 group are applied. Since the target in Fig. 3 does not possess rotation symmetry, rotating the target 90° will almost certainly result in a dissimilar bistatic observation. In this case, the bistatic measurement is not invariant over operations of the \mathcal{C}_4 group, since the target does not possess \mathcal{C}_4 symmetry.

This invariance in bistatic scattering suggests a method for discriminating between objects with geometric symmetries (e.g., mines) and those without (e.g., clutter). Of course, buried objects cannot be rotated or reflected to evaluate the invariance of a bistatic observation. However, rotating or reflecting an object with respect to a bistatic antenna pair is equivalent to rotating or reflecting the bistatic antenna pair with respect to the object, the difference simply being the local coordinate system considered fixed. For example, consider the case shown

in Fig. 3(b). A pair of bistatic elements is reflected across the plane of target symmetry; since this operation is identical to reflecting the object with respect to the bistatic elements, the two bistatic measurements will be equal (to within measurement error).

Likewise, this concept can be applied to subsurface targets with higher orders of symmetry. All the geometric operations of a point group of order N can alternatively be applied to the geometry of a single bistatic observation. The result will be the geometries for $N - 1$ new bistatic observations (the identity operation, by definition, results in the original bistatic geometry). If the observed target also possesses the symmetry of this group, then each of these bistatic observations will result in equal measurements. Conversely, the set of $N - 1$ bistatic measurements will almost certainly be dissimilar if the subsurface target is asymmetric. This result illustrates the strength of group theory and why it is applied in a wide variety of applications. Once one solution is found, the solution for many other problems can be determined by applying the operations of a relevant group. Perhaps more important, group theory also allows for the systematic identification of all such solutions.

In addition to the geometric operations of rotation and reflection, another operation is relevant when considering bistatic measurements. Say, for example, that the source and sensor are *transposed*, so the transmitter is attached to the receive antenna and vice versa. From a group-theoretic perspective, we can view this operation as a permutation of the source and sensor, and thus can describe the two bistatic geometries (the original and its transpose) as being related by the operations of the second-order permutation group \mathcal{S}_2 . Assuming the antennas, the scatterer, and its surrounding media consist of simple (i.e., linear and isotropic) material, electromagnetic reciprocity requires that the two bistatic observations be equal. Thus, we can say a bistatic measurement is invariant under the operations of group \mathcal{S}_2 . However, unlike the operations of other point groups, this measurement invariance is independent of the observed object: the invariance is observed for both symmetric and asymmetric scatterers.

TABLE I
ELEMENT MULTIPLICATION TABLE OF THE BISTATIC GROUP X_{4ar}

	g_0	g_1	g_2	g_3	g_4	g_5	g_6	g_7	g_8	g_9	g_{10}	g_{11}	g_{12}	g_{13}	g_{14}	g_{15}
g_0	g_0	g_1	g_2	g_3	g_4	g_5	g_6	g_7	g_8	g_9	g_{10}	g_{11}	g_{12}	g_{13}	g_{14}	g_{15}
g_1	g_1	g_4	g_5	g_6	g_7	g_8	g_9	g_0	g_{10}	g_{11}	g_2	g_3	g_{13}	g_{14}	g_{15}	g_{12}
g_2	g_2	g_{10}	g_0	g_{12}	g_8	g_7	g_{15}	g_5	g_4	g_{14}	g_1	g_{13}	g_3	g_{11}	g_9	g_6
g_3	g_3	g_6	g_{12}	g_0	g_9	g_{13}	g_1	g_{11}	g_{14}	g_4	g_{15}	g_7	g_2	g_5	g_8	g_{10}
g_4	g_4	g_7	g_8	g_9	g_0	g_{10}	g_{11}	g_1	g_2	g_3	g_5	g_6	g_{14}	g_{15}	g_{12}	g_{13}
g_5	g_5	g_2	g_1	g_{13}	g_{10}	g_0	g_{12}	g_8	g_7	g_{15}	g_4	g_{14}	g_6	g_3	g_{11}	g_9
g_6	g_6	g_9	g_{13}	g_1	g_{11}	g_{14}	g_4	g_3	g_{15}	g_7	g_{12}	g_0	g_5	g_8	g_{10}	g_2
g_7	g_7	g_0	g_{10}	g_{11}	g_1	g_2	g_3	g_4	g_5	g_6	g_8	g_9	g_{15}	g_{12}	g_{13}	g_{14}
g_8	g_8	g_5	g_4	g_{14}	g_2	g_1	g_{13}	g_{10}	g_0	g_{12}	g_7	g_{15}	g_9	g_6	g_3	g_{11}
g_9	g_9	g_{11}	g_{14}	g_4	g_3	g_{15}	g_7	g_6	g_{12}	g_0	g_{13}	g_1	g_8	g_{10}	g_2	g_5
g_{10}	g_{10}	g_8	g_7	g_{15}	g_5	g_4	g_{14}	g_2	g_1	g_{13}	g_0	g_{12}	g_{11}	g_9	g_6	g_3
g_{11}	g_{11}	g_3	g_{15}	g_7	g_6	g_{12}	g_0	g_9	g_{13}	g_1	g_{14}	g_4	g_{10}	g_2	g_5	g_8
g_{12}	g_{12}	g_{15}	g_3	g_2	g_{14}	g_{11}	g_{10}	g_{13}	g_9	g_8	g_6	g_5	g_0	g_7	g_4	g_1
g_{13}	g_{13}	g_{12}	g_6	g_5	g_{15}	g_3	g_2	g_{14}	g_{11}	g_{10}	g_9	g_8	g_1	g_0	g_7	g_4
g_{14}	g_{14}	g_{13}	g_9	g_8	g_{12}	g_6	g_5	g_{15}	g_3	g_2	g_{11}	g_{10}	g_4	g_1	g_0	g_7
g_{15}	g_{15}	g_{14}	g_{11}	g_{10}	g_{13}	g_9	g_8	g_{12}	g_6	g_5	g_3	g_2	g_7	g_4	g_1	g_0

A. Generation of Bistatic Group C_{Mar}

These three basic operations (reflection, rotation, and transpose) can be combined to form another discrete point group, one that describes the symmetry of the electromagnetic field scattered from a symmetric object. In the nomenclature of group theory, these three operations are group *generators*—all the elements of the resulting group can be completely expressed as a series of these basic operations [20]. For example, a rotation of $\phi_M = 2\pi/M$ is a generator for the cyclic group C_M . Symbolically denoting this operation as C_M , we can represent a sequence of m rotations as C_M^m , resulting in a total rotation angle of $\phi = m2\pi/M$. The elements of the M -order cyclic group can thus be completely expressed in terms of terms of the generator operation C_M

$$C_M = \{e, C_M, C_M^2, C_M^3, \dots, C_M^{M-1}\}. \tag{1}$$

The symbol e represents the identity operation, a required element for all groups. This identity operation can likewise be expressed in terms of the generator operation C_M as $e = C_M^M$, an operation corresponding to a full rotation of 2π rad. Similarly, we can denote the reflection operation as σ_a , and since $e = \sigma_a^2$ (i.e., a sequence of two reflections returns the object to its original state), this operation generates the elements of the reflection group $\mathcal{R} = \{e, \sigma_a\}$. Additionally, denoting the transpose operation as π , the elements of a second-order permutation group (\mathcal{S}_2) are created, where $\mathcal{S}_2 = \{e, \pi\}$ and $e = \pi^2$.

The set of generators $\{C_M, \sigma_a, \pi\}$ can also be used in combination to form a group, which is described as the *adjoined*

group of C_M , \mathcal{R} , and \mathcal{S}_2 . Adjoining two groups will result in a new group whose order is the product of the order of each original group. For example, the group C_{Ma} is formed by adjoining group C_M (order M) and \mathcal{R} (order 2) and thus has order $2M$. Further adjoining C_{Ma} with \mathcal{S}_2 produces a new group of order $4M$, which, using the notation of Baum [12], we denote as C_{Mar} . The group C_{Mar} is formed using the generators C_M , σ_a , and π in combination. Since a bistatic observation of an object with C_{Ma} symmetry (or higher) will remain invariant under all $4M$ operations of group C_{Mar} , we will refer to C_{Mar} as the bistatic group.

For example, consider the bistatic group C_{4ar} . This group, which is formed with generator C_4 (a $\pi/2$ rotation), consists of 16 elements, representing all unique combinations of reflections, rotations, and permutations. Table I provides a description of each element in the group in terms of generators σ_a , C_4 , and π . Likewise, Table II shows the multiplication table for these group elements. Note that the group is not commutative, so that the table must be interpreted as the product of the row element followed by the column element (e.g., $g_6g_5 = g_{14} \neq g_5g_6$).

B. Bistatic Group Representation

A matrix *representation* of any group order N can be formed with a set of N matrices \vec{g}_n . Each matrix of this representation must correspond to an element g_n of the group, and the matrices must follow the group multiplication table, such that if $g_i g_j = g_k$, then $\vec{g}_i \vec{g}_j = \vec{g}_k$. From the definition of a group, it is evident that a representation must consist of square, nonsingular matrices. In a procedure analogous to identifying the

TABLE II
ELEMENTS OF BISTATIC GROUP X_{4ar} , REPRESENTED IN TERMS
OF GENERATOR OPERATIONS σ_a , C_4 , AND π

$\mathbf{g}_0 = \mathbf{g}_0^{-1} = e$
$\mathbf{g}_1 = \mathbf{g}_7^{-1} = C_4$
$\mathbf{g}_2 = \mathbf{g}_2^{-1} = \sigma$
$\mathbf{g}_3 = \mathbf{g}_3^{-1} = \pi$
$\mathbf{g}_4 = \mathbf{g}_4^{-1} = C_4^2$
$\mathbf{g}_5 = \mathbf{g}_5^{-1} = C_4 \sigma$
$\mathbf{g}_6 = \mathbf{g}_{11}^{-1} = C_4 \pi$
$\mathbf{g}_7 = \mathbf{g}_1^{-1} = C_4^3$
$\mathbf{g}_8 = \mathbf{g}_8^{-1} = C_4^2 \sigma$
$\mathbf{g}_9 = \mathbf{g}_9^{-1} = C_4^2 \pi$
$\mathbf{g}_{10} = \mathbf{g}_{10}^{-1} = C_4^3 \sigma$
$\mathbf{g}_{11} = \mathbf{g}_6^{-1} = C_4^3 \pi$
$\mathbf{g}_{12} = \mathbf{g}_{12}^{-1} = \sigma \pi$
$\mathbf{g}_{13} = \mathbf{g}_{13}^{-1} = \pi C_4 \sigma$
$\mathbf{g}_{14} = \mathbf{g}_{14}^{-1} = \pi C_4^2 \sigma$
$\mathbf{g}_{15} = \mathbf{g}_{15}^{-1} = \sigma C_4 \pi$

elements of group C_{4ar} using group generators, a matrix representation of the bistatic group can be formed using matrix generators. We begin by defining three 6×6 matrices \vec{C}_M , $\vec{\sigma}_a$, and $\vec{\pi}$ as follows:

$$\begin{aligned}
 \vec{C}_M &= \begin{bmatrix} \cos\left(\frac{2\pi}{M}\right) & -\sin\left(\frac{2\pi}{M}\right) & 0 & 0 & 0 & 0 \\ \sin\left(\frac{2\pi}{M}\right) & \cos\left(\frac{2\pi}{M}\right) & 0 & 0 & 0 & 0 \\ 0 & 0 & 1 & 0 & 0 & 0 \\ 0 & 0 & 0 & \cos\left(\frac{2\pi}{M}\right) & -\sin\left(\frac{2\pi}{M}\right) & 0 \\ 0 & 0 & 0 & \sin\left(\frac{2\pi}{M}\right) & \cos\left(\frac{2\pi}{M}\right) & 0 \\ 0 & 0 & 0 & 0 & 0 & 1 \end{bmatrix} \\
 \vec{\sigma}_a &= \begin{bmatrix} -1 & 0 & 0 & 0 & 0 & 0 \\ 0 & 1 & 0 & 0 & 0 & 0 \\ 0 & 0 & 1 & 0 & 0 & 0 \\ 0 & 0 & 0 & -1 & 0 & 0 \\ 0 & 0 & 0 & 0 & 1 & 0 \\ 0 & 0 & 0 & 0 & 0 & 1 \end{bmatrix} \\
 \vec{\pi} &= \begin{bmatrix} 0 & 0 & 0 & 1 & 0 & 0 \\ 0 & 0 & 0 & 0 & 1 & 0 \\ 0 & 0 & 0 & 0 & 0 & 1 \\ 1 & 0 & 0 & 0 & 0 & 0 \\ 0 & 1 & 0 & 0 & 0 & 0 \\ 0 & 0 & 1 & 0 & 0 & 0 \end{bmatrix}.
 \end{aligned} \tag{2}$$

Multiplying $\vec{\sigma}_a$ with itself results in a 6×6 identity matrix, denoted as \vec{e} . Thus, it is apparent the matrices $\vec{\sigma}_a$ and \vec{e} form a second-order group. The multiplication table for this group is

identical to that of \mathcal{R} , provided that matrix \vec{e} corresponds to operation e , and $\vec{\sigma}_a$ to σ_a . The matrices \vec{e} and $\vec{\sigma}_a$, therefore, form a matrix representation group \mathcal{R} . In a similar manner, the matrix $\vec{\pi}$ (where $\vec{\pi}\vec{\pi} = \vec{e}$) can form a representation of \mathcal{S}_2 , and powers of \vec{C}_M (where $\vec{C}_M^M = \vec{e}$) form a representation of C_M .

A matrix representation of the bistatic group C_{Mar} is likewise formed from all possible products of the matrix generators \vec{C}_M , $\vec{\sigma}_a$, and $\vec{\pi}$. A total of $4M$ distinct matrices are formed from these products, each one representing one of the $4M$ elements of C_{Mar} . Each matrix \vec{g}_n is expressed in terms of the generator matrices in precisely the same form that each element g_n is expressed in terms of the group generators. For example, for group C_{4ar} we note from Table I that $g_{13} = C_4 \sigma_a \pi$, therefore $\vec{g}_{13} = \vec{C}_4 \vec{\sigma}_a \vec{\pi}$. The complete set of 16 matrices \vec{g}_n forms a matrix representation group C_{4ar} . Accordingly, the multiplication table presented in Table I likewise expresses the matrix products of \vec{g}_n (i.e., if $g_i g_j = g_k$ then $\vec{g}_i \vec{g}_j = \vec{g}_k$).

Matrix representations are often used in group theory to study the properties of a group. By examining the properties of the matrices (e.g., the trace) that form representations of a group, the structure and characteristics of a group and/or its elements can be quantified. Matrix representations are likewise helpful if they have a direct physical interpretation, which is specifically why the generators described in (2) were chosen. The resulting matrix representation of C_{Mar} is by no means unique; much simpler representations can be formed with matrices of smaller dimension. However, this particular representation provides a physical interpretation of the group operations that will be useful in the mathematical analysis of Section IV.

IV. BISTATIC SCATTERING DYADIC

Group theory provides an elegant mathematical structure to describe and examine the effects of target and sensor symmetry on bistatic scattering observations. However, its usefulness in engineering applications is perhaps dependent on its ability to reveal solutions that are not otherwise obvious. In this section, the matrix representation of the bistatic group C_{Mar} will be used to define the general response of a symmetric scatterer completely, including all dependent responses in terms of both spatial location and polarization. The results will be similar in form to that provided by reciprocity, but significantly more extensive.

The scattered electric field $\vec{E}(\vec{r})$ from a linear, isotropic, time-invariant target, illuminated by an electric current density $\vec{J}(\vec{r}, t)$, is expressed as

$$\vec{E}(\vec{r}; t) = \int_{-\infty}^{\infty} \int_V \vec{G}(\vec{r}, \vec{r}'; t - t') \vec{J}(\vec{r}'; t') dV' dt' \tag{3}$$

or, if the source is represented in the frequency domain, as

$$\vec{E}(\vec{r}; \omega) = \int_V \vec{G}(\vec{r}, \vec{r}'; \omega) \vec{J}(\vec{r}'; \omega) dV' \tag{4}$$

where $\vec{G}(\vec{r}, \vec{r}'; t - t')$ represents the dyadic Green's function of the scatterer. This dyadic function completely describes the scattering response of the buried target as a function of time/frequency, spatial location, and polarization. In addition to the size,

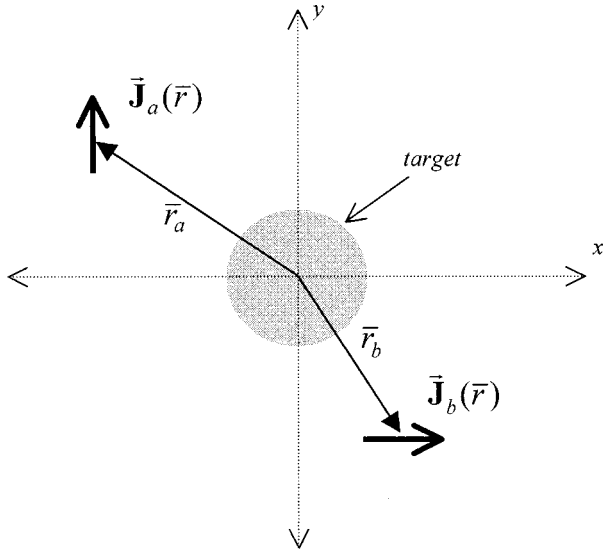


Fig. 4. Description of the bistatic measurement geometry for subsurface sensing. The surface lies on the plane $z = 0$. Therefore, the target is located below this plane ($z < 0$), while the antenna elements $\vec{\mathbf{J}}_a(\vec{r})$ and $\vec{\mathbf{J}}_b(\vec{r})$ are located above ($z > 0$).

shape, and material of the scatterer, the dyadic Green's function of a buried target is also dependent on the target's depth and the electromagnetic properties of the surrounding medium.

The dyadic Green's function $\vec{\mathbf{G}}(\vec{r}, \vec{r}')$ (the time/frequency variable will be suppressed for the remainder of the paper) can be represented as a 3×3 matrix of independent scalar functions

$$\vec{\mathbf{G}}(\vec{r}, \vec{r}') = \begin{bmatrix} s_{xx}(\vec{r}, \vec{r}') & s_{xy}(\vec{r}, \vec{r}') & s_{xz}(\vec{r}, \vec{r}') \\ s_{yx}(\vec{r}, \vec{r}') & s_{yy}(\vec{r}, \vec{r}') & s_{yz}(\vec{r}, \vec{r}') \\ s_{zx}(\vec{r}, \vec{r}') & s_{zy}(\vec{r}, \vec{r}') & s_{zz}(\vec{r}, \vec{r}') \end{bmatrix}. \quad (5)$$

Since the electromagnetic detection of shallow subsurface objects is inherently a near-field problem, no further simplification of this matrix can be applied. Specifically, this matrix cannot be reduced to a 2×2 matrix with a transformation of the coordinate system (e.g., \hat{v} and \hat{h}): $\vec{\mathbf{G}}(\vec{r}, \vec{r}')$ is assumed to be full rank. For a given scatterer, the nine scalar functions of $\vec{\mathbf{G}}(\vec{r}, \vec{r}')$ can be determined either by an electromagnetic calculation or by measurement. In general, neither technique is easily accomplished. However, group-theoretic techniques can be particularly helpful in reducing this difficulty, provided the target displays geometric symmetry. For this case, the scalar functions of $\vec{\mathbf{G}}(\vec{r}, \vec{r}')$ are related, such that one solution can be used to determine several others. Group theory provides a tool for identifying all such relations and solutions.

A. Generalized Reciprocity for Symmetric Targets

Consider Fig. 4, showing a scatterer in the presence of two electric current elements, described as $\vec{\mathbf{J}}_a(\vec{r})$ and $\vec{\mathbf{J}}_b(\vec{r})$. With this geometry, we can consider two bistatic observations: either $\vec{\mathbf{J}}_a(\vec{r})$ is the source and $\vec{\mathbf{J}}_b(\vec{r})$ the sensor, or the reciprocal case where $\vec{\mathbf{J}}_b(\vec{r})$ is the source and $\vec{\mathbf{J}}_a(\vec{r})$ the sensor. From reciprocity, we know that the reaction of the scattered field $\vec{\mathbf{E}}_a(\vec{r})$

[from source $\vec{\mathbf{J}}_a(\vec{r})$] with $\vec{\mathbf{J}}_b(\vec{r})$ equal to the reaction of $\vec{\mathbf{E}}_a(\vec{r})$ with $\vec{\mathbf{J}}_a(\vec{r})$

$$\iint_{V_a} \vec{\mathbf{J}}_a(\vec{r}) \cdot \vec{\mathbf{E}}_b(\vec{r}) dV = \iint_{V_b} \vec{\mathbf{J}}_b(\vec{r}) \cdot \vec{\mathbf{E}}_a(\vec{r}) dV. \quad (6)$$

Defining the reaction operation as $\langle \vec{\mathbf{J}}(\vec{r}) \cdot \vec{\mathbf{E}}(\vec{r}) \rangle$, (4) and (6) can be combined to express reciprocity as

$$\begin{aligned} \iint_V \langle \vec{\mathbf{J}}_a(\vec{r}) \cdot \vec{\mathbf{G}}(\vec{r}, \vec{r}') \vec{\mathbf{J}}_b(\vec{r}') \rangle dV \\ = \iint_V \langle \vec{\mathbf{J}}_b(\vec{r}) \cdot \vec{\mathbf{G}}(\vec{r}, \vec{r}') \vec{\mathbf{J}}_a(\vec{r}') \rangle dV. \end{aligned} \quad (7)$$

Since (7) is true for all current densities and scatterers, it follows that the dyadic Green's function must satisfy the expression [21]

$$\vec{\mathbf{G}}(\vec{r}, \vec{r}') = \vec{\mathbf{G}}^T(\vec{r}', \vec{r}). \quad (8)$$

To simplify the analysis, we assume that the current elements are Hertzian dipoles, located at positions \vec{r}_a and \vec{r}_b . The reciprocity expression (7) is therefore

$$\vec{\mathbf{J}}_a(\vec{r}_a) \cdot \vec{\mathbf{G}}(\vec{r}_a, \vec{r}_b) \vec{\mathbf{J}}_b(\vec{r}_b) = \vec{\mathbf{J}}_b(\vec{r}_b) \cdot \vec{\mathbf{G}}(\vec{r}_b, \vec{r}_a) \vec{\mathbf{J}}_a(\vec{r}_a) \quad (9)$$

where $\vec{\mathbf{G}}(\vec{r}_b, \vec{r}_a) = \vec{\mathbf{G}}^T(\vec{r}_a, \vec{r}_b)$.

Consider now the case where the scatterer possesses \mathcal{C}_{Ma} symmetry. As discussed previously, applying any operation of the bistatic group \mathcal{C}_{Mar} to the dipole geometry will leave the electromagnetic response unchanged. The reaction values of (9) are, therefore, invariant with respect to all operations of the bistatic group, when applied to current densities $\vec{\mathbf{J}}_a(\vec{r})$ and $\vec{\mathbf{J}}_b(\vec{r})$, i.e.,

$$\begin{aligned} \alpha_a(\vec{r}_a, \vec{r}_b) &\equiv \vec{\mathbf{J}}_a(\vec{r}_a) \cdot \vec{\mathbf{G}}(\vec{r}_a, \vec{r}_b) \vec{\mathbf{J}}_b(\vec{r}_b) \\ &= g_n \left\{ \vec{\mathbf{J}}_a(\vec{r}_a) \right\} \cdot \vec{\mathbf{G}}(\vec{r}_a, \vec{r}_b) g_n \left\{ \vec{\mathbf{J}}_b(\vec{r}_b) \right\} \end{aligned} \quad (10)$$

and

$$\begin{aligned} \alpha_b(\vec{r}_b, \vec{r}_a) &\equiv \vec{\mathbf{J}}_b(\vec{r}_b) \cdot \vec{\mathbf{G}}(\vec{r}_b, \vec{r}_a) \vec{\mathbf{J}}_a(\vec{r}_a) \\ &= g_n \left\{ \vec{\mathbf{J}}_b(\vec{r}_b) \right\} \cdot \vec{\mathbf{G}}(\vec{r}_b, \vec{r}_a) g_n \left\{ \vec{\mathbf{J}}_a(\vec{r}_a) \right\} \end{aligned} \quad (11)$$

where $g_n \{ \}$ indicates that the geometric operation of group element g_n is applied. If each reaction α_a and α_b is invariant with respect to the operations of the bistatic group, then the sum of the values is likewise invariant. This resulting invariant value can be compactly expressed by defining the six-dimensional (6-D) position vector $\vec{\mathbf{R}}$

$$\vec{\mathbf{R}} \equiv [\vec{r}_a^T, \vec{r}_b^T]^T \quad (12)$$

as well as the 6-D vector $\vec{\mathbf{J}}\vec{\mathbf{R}}$

$$\vec{\mathbf{J}}(\vec{\mathbf{R}}) \equiv \left[\vec{\mathbf{J}}_a^T(\vec{r}_a), \vec{\mathbf{J}}_b^T(\vec{r}_b) \right]^T. \quad (13)$$

The two vectors $\vec{\mathbf{R}}$ and $\vec{\mathbf{J}}\vec{\mathbf{R}}$ completely define a bistatic measurement geometry, specifying both dipole location and orientation. Using these definitions, we define the scalar value $\alpha(\vec{\mathbf{R}})$ as

$$\alpha(\vec{\mathbf{R}}) \equiv \vec{\mathbf{J}}(\vec{\mathbf{R}}) \cdot \vec{\mathbf{G}}(\vec{\mathbf{R}}) \vec{\mathbf{J}}(\vec{\mathbf{R}}) = \alpha_a(\vec{r}_a, \vec{r}_b) + \alpha_b(\vec{r}_b, \vec{r}_a) \quad (14)$$

where $\vec{\mathcal{G}}(\vec{\mathbf{R}})$ is a 6×6 matrix given as

$$\begin{aligned} \vec{\mathcal{G}}(\vec{\mathbf{R}}) &\equiv \begin{bmatrix} 0 & \vec{\mathbf{G}}(\vec{r}_a, \vec{r}_b) \\ \vec{\mathbf{G}}(\vec{r}_b, \vec{r}_a) & 0 \end{bmatrix} \\ &= \begin{bmatrix} 0 & \vec{\mathbf{G}}^T(\vec{r}_b, \vec{r}_a) \\ \vec{\mathbf{G}}(\vec{r}_b, \vec{r}_a) & 0 \end{bmatrix}. \end{aligned} \quad (15)$$

For a scatter possessing \mathcal{C}_{Ma} symmetry, the invariance of $\alpha(\vec{\mathbf{R}})$ with respect to the operations of \mathcal{C}_{Mar} is stated as

$$\begin{aligned} \alpha(\vec{\mathbf{R}}) &= \vec{\mathcal{J}}(\vec{\mathbf{R}}) \cdot \vec{\mathcal{G}}(\vec{\mathbf{R}}) \vec{\mathcal{J}}(\vec{\mathbf{R}}) \\ &= g_n \left\{ \vec{\mathcal{J}}(\vec{\mathbf{R}}) \right\} \cdot \vec{\mathcal{G}}(\vec{\mathbf{R}}) g_n \left\{ \vec{\mathcal{J}}(\vec{\mathbf{R}}) \right\} \end{aligned} \quad (16)$$

where $g_n \left\{ \vec{\mathcal{J}}(\vec{\mathbf{R}}) \right\}$ defines the bistatic geometry after the locations and orientations of the dipole elements have been transformed by the n th element of group \mathcal{C}_{Mar} . We denote this new geometry as $\vec{\mathcal{J}}_n(\vec{\mathbf{R}})$, so that

$$\vec{\mathcal{J}}_n(\vec{\mathbf{R}}_n) \equiv g_n \left\{ \vec{\mathcal{J}}(\vec{\mathbf{R}}) \right\}. \quad (17)$$

Since (17) describes a linear operation on vectors $\vec{\mathbf{R}}$ and $\vec{\mathcal{J}}$ that, likewise, result in vectors $\vec{\mathbf{R}}_n$ and $\vec{\mathcal{J}}_n$, the operation g_n can alternatively be expressed as a matrix multiplication, i.e.,

$$\vec{\mathbf{R}}_n = g_n \left\{ \vec{\mathbf{R}} \right\} = \vec{\mathbf{g}}_n \vec{\mathbf{R}} \text{ and } \vec{\mathcal{J}}_n = g_n \left\{ \vec{\mathcal{J}} \right\} = \vec{\mathbf{g}}_n \vec{\mathcal{J}}. \quad (18)$$

In other words, the locations of the dipole elements are transformed by the operation $\vec{\mathbf{R}}_n = \vec{\mathbf{g}}_n \vec{\mathbf{R}}$, whereas the direction of $\vec{\mathcal{J}}(\vec{\mathbf{R}})$ is modified by the operation $\vec{\mathcal{J}}_n = \vec{\mathbf{g}}_n \vec{\mathcal{J}}$. For the bistatic group \mathcal{C}_{Mar} , the set of matrices $\vec{\mathbf{g}}_n$ that satisfy (18) is identical to the set that forms the matrix representation of \mathcal{C}_{Mar} presented in Section III [generated from the matrices defined in (2)]. For example, again consider the bistatic group $\mathcal{C}_{4\text{ar}}$. A rotation of the bistatic geometry by $\pi/2$ rad will result in new dipole locations $\vec{\mathbf{R}}_1 = g_1 \left\{ \vec{\mathbf{R}} \right\} = \vec{\mathbf{g}}_1 \vec{\mathbf{R}} = \vec{\mathbf{C}}_4 \vec{\mathbf{R}}$, as well as new dipole orientations $\vec{\mathcal{J}}_1 = g_1 \left\{ \vec{\mathcal{J}} \right\} = \vec{\mathbf{g}}_1 \vec{\mathcal{J}} = \vec{\mathbf{C}}_4 \vec{\mathcal{J}}$. The remainder of the matrices $\vec{\mathbf{g}}_n$ in this representation can, likewise, be shown to provide the geometric operation associated with group element g_n . Recall that this matrix representation is not unique: it was constructed specifically so that the elements $\vec{\mathbf{g}}_n$ would satisfy (18).

From (18), it is apparent that (17) can be written as

$$\vec{\mathcal{J}}_n(\vec{\mathbf{R}}_n) \equiv g_n \left\{ \vec{\mathcal{J}}(\vec{\mathbf{R}}) \right\} = \vec{\mathbf{g}}_n \vec{\mathcal{J}}(\vec{\mathbf{g}}_n^{-1} \vec{\mathbf{R}}_n). \quad (19)$$

Combining (16) and (19), we can write the function $\alpha(\vec{\mathbf{R}})$ as

$$\begin{aligned} \vec{\mathcal{J}}(\vec{\mathbf{R}}) \cdot \vec{\mathcal{G}}(\vec{\mathbf{R}}) \vec{\mathcal{J}}(\vec{\mathbf{R}}) &= \vec{\mathcal{J}}_n(\vec{\mathbf{R}}_n) \cdot \vec{\mathcal{G}}(\vec{\mathbf{R}}_n) \vec{\mathcal{J}}_n(\vec{\mathbf{R}}_n) \\ &= \vec{\mathbf{g}}_n \vec{\mathcal{J}}(\vec{\mathbf{g}}_n^{-1} \vec{\mathbf{R}}_n) \cdot \vec{\mathcal{G}}(\vec{\mathbf{R}}_n) \vec{\mathbf{g}}_n \\ &\quad \times \vec{\mathcal{J}}(\vec{\mathbf{g}}_n^{-1} \vec{\mathbf{R}}_n) \\ &= \vec{\mathcal{J}}(\vec{\mathbf{R}}) \cdot \vec{\mathbf{g}}_n^T \vec{\mathcal{G}}(\vec{\mathbf{g}}_n \vec{\mathbf{R}}) \vec{\mathbf{g}}_n \vec{\mathcal{J}}(\vec{\mathbf{R}}). \end{aligned} \quad (20)$$

Since this relationship is valid for all scatterers and dipoles, it follows that

$$\vec{\mathcal{G}}(\vec{\mathbf{R}}) = \vec{\mathbf{g}}_n^T \vec{\mathcal{G}}(\vec{\mathbf{g}}_n \vec{\mathbf{R}}) \vec{\mathbf{g}}_n. \quad (21)$$

Therefore we have

$$\vec{\mathcal{G}}(\vec{\mathbf{g}}_n \vec{\mathbf{R}}) = \vec{\mathbf{g}}_n^{-T} \vec{\mathcal{G}}(\vec{\mathbf{R}}) \vec{\mathbf{g}}_n^{-1} \quad n = 0, 1, 2, \dots, N-1. \quad (22)$$

Thus, from a given solution of the dyadic Green's function $\vec{\mathcal{G}}(\vec{r}, \vec{r}')$, as represented by $\vec{\mathcal{G}}(\vec{\mathbf{R}})$, $N-1$ other solutions $\vec{\mathcal{G}}(\vec{\mathbf{g}}_n \vec{\mathbf{R}})$ can be determined from (22). Likewise, extracting the dyadic Green's function from $\vec{\mathcal{G}}(\vec{\mathbf{g}}_n \vec{\mathbf{R}})$ using (15), $N-1$ new solutions, denoted as $\vec{\mathcal{G}}(\vec{r}, \vec{r}'_n)$, can be derived. The group-theoretic approach ensures that this set of solutions is closed, i.e., there are no other solutions that can be determined from $\vec{\mathcal{G}}(\vec{r}, \vec{r}')$.

For example, applying (21) using element g_{13} of group $\mathcal{C}_{4\text{ar}}$, we can determine the following relation:

$$\begin{aligned} \vec{\mathcal{G}}(\vec{r}_{13}, \vec{r}'_{13}) &= \begin{bmatrix} g_{yy}(\vec{r}, \vec{r}') & g_{xy}(\vec{r}, \vec{r}') & -g_{zy}(\vec{r}, \vec{r}') \\ g_{yx}(\vec{r}, \vec{r}') & g_{xx}(\vec{r}, \vec{r}') & -g_{zx}(\vec{r}, \vec{r}') \\ -g_{yz}(\vec{r}, \vec{r}') & -g_{xz}(\vec{r}, \vec{r}') & g_{zz}(\vec{r}, \vec{r}') \end{bmatrix} \end{aligned} \quad (23)$$

where vectors \vec{r}_{13} and \vec{r}'_{13} define the bistatic geometry resulting from the application of operation g_{13} on \vec{r} and \vec{r}' , an operation consisting of a rotation, reflection, and transpose. Equation (23) indicates, for example, that $g_{xx}(\vec{r}_{13}, \vec{r}'_{13}) = g_{yy}(\vec{r}, \vec{r}')$ and $g_{zx}(\vec{r}_{13}, \vec{r}'_{13}) = -g_{yz}(\vec{r}, \vec{r}')$. These relationships are similar to those resulting from reciprocity [e.g., $g_{xy}(\vec{r}', \vec{r}) = g_{yx}(\vec{r}, \vec{r}')$]. Therefore, (22) can be thought of as a more general form of electromagnetic reciprocity, applicable specifically to symmetric targets.

B. Degenerate Scattering Solutions

For the backscattering geometry, where $\vec{r} = \vec{r}'$, the reciprocity relationship of (8) specifies that symmetric off-diagonal elements of $\vec{\mathcal{G}}(\vec{r}, \vec{r}')$ must be equal, regardless of the scattering target. For symmetric targets, similar relationships can be found for other specific scattering geometries. Group-theoretic techniques can be used, first to determine these scattering geometries, and then determine the resulting form of $\vec{\mathcal{G}}(\vec{r}, \vec{r}')$. This is accomplished by examining the *degenerate* cases of the group representation. A degenerate case occurs when the operations of two or more group elements provide an identical result—these elements are thus equivalent for a degenerate case. For example, a bistatic geometry $\vec{\mathbf{R}}$ would be considered degenerate if there were two (or more) different elements $\vec{\mathbf{g}}_n$ such that

$$\vec{\mathbf{g}}_i \vec{\mathbf{R}} = \vec{\mathbf{g}}_j \vec{\mathbf{R}} \text{ where } i \neq j. \quad (24)$$

In other words, a geometry is considered degenerate if it can be related to a second geometry by two (or more) dissimilar group operations. Note that since the inverse of a group element must also be an element of the group, this second geometry is also degenerate.

Using (24) we can define degenerate geometries as those vectors \vec{r} that satisfy the equation

$$\vec{\mathbf{R}} = \vec{\mathbf{g}}_i^{-1} \vec{\mathbf{g}}_j \vec{\mathbf{R}} \text{ where } i \neq j. \quad (25)$$

It is apparent from (25) that eigenvectors of $\vec{\mathbf{g}}_i^{-1} \vec{\mathbf{g}}_j$ with unit-valued (i.e., $\lambda = 1$) eigenvalues define degenerate bistatic ge-

ometries. It also appears that for a group of order N there are $N(N-1)$ matrices $\overset{\leftrightarrow}{\mathbf{g}}_i \overset{\leftrightarrow}{\mathbf{g}}_j$ (with $i \neq j$). However, the matrices $\overset{\leftrightarrow}{\mathbf{g}}_n$ represent a group. Therefore, the matrix $\overset{\leftrightarrow}{\mathbf{g}}_i \overset{\leftrightarrow}{\mathbf{g}}_j$ is a group element, as is $\overset{\leftrightarrow}{\mathbf{g}}_n^{-1}$. As a result, every matrix $\overset{\leftrightarrow}{\mathbf{g}}_i \overset{\leftrightarrow}{\mathbf{g}}_j$ is equal to one of the N matrix elements $\overset{\leftrightarrow}{\mathbf{g}}_n$, and thus (25) can be effectively written as

$$\bar{\mathbf{R}}_{dn} = \overset{\leftrightarrow}{\mathbf{g}}_n \bar{\mathbf{R}}_{dn} \quad (26)$$

where $\bar{\mathbf{R}}_{dn}$ denotes a degenerate geometry derived from matrix $\overset{\leftrightarrow}{\mathbf{g}}_n$.

It is apparent from (26) that each eigenvector of matrix $\overset{\leftrightarrow}{\mathbf{g}}_n$ with a unit-valued eigenvalue describes a degenerate bistatic geometry $\bar{\mathbf{r}}_{dn}$, as does any linear combination of these eigenvectors. The resulting bistatic geometry is degenerate with respect to any two dissimilar group operations $\overset{\leftrightarrow}{\mathbf{g}}_i$ and $\overset{\leftrightarrow}{\mathbf{g}}_j$ where $\overset{\leftrightarrow}{\mathbf{g}}_i \overset{\leftrightarrow}{\mathbf{g}}_j = \overset{\leftrightarrow}{\mathbf{g}}_n$. Perhaps the easiest way to interpret a degenerate geometry is to evaluate (25) for the case where $\overset{\leftrightarrow}{\mathbf{g}}_i$ is the identity operation (i.e., $\overset{\leftrightarrow}{\mathbf{g}}_i = \overset{\leftrightarrow}{\mathbf{e}}$). In this case, (25) reduces to (26) if $\overset{\leftrightarrow}{\mathbf{g}}_j = \overset{\leftrightarrow}{\mathbf{g}}_n$, meaning that the eigenvalues of $\overset{\leftrightarrow}{\mathbf{g}}_n$ form geometries that are degenerate with respect to operations $\overset{\leftrightarrow}{\mathbf{g}}_0 = \overset{\leftrightarrow}{\mathbf{e}}$ and $\overset{\leftrightarrow}{\mathbf{g}}_n$. In other words, a geometry produced from the eigenvalues of matrix $\overset{\leftrightarrow}{\mathbf{g}}_n$ will not be modified by the operation g_n : for the degenerate geometry, g_n is equivalent to the identity operation e .

Combining (22) and (26), we form the result

$$\overset{\leftrightarrow}{\mathbf{G}}(\bar{\mathbf{R}}_{dn}) = \overset{\leftrightarrow}{\mathbf{g}}_n^{-T} \overset{\leftrightarrow}{\mathbf{G}}(\bar{\mathbf{R}}_{dn}) \overset{\leftrightarrow}{\mathbf{g}}_n^{-1} \quad (27)$$

From this expression, the general form of the dyadic Green's function $\overset{\leftrightarrow}{\mathbf{G}}(\bar{\mathbf{r}}, \bar{\mathbf{r}}'_n)$ can be determined for all degenerate geometries. For example, matrix $\overset{\leftrightarrow}{\mathbf{g}}_6$ of the group \mathcal{C}_{4ar} has just one eigenvector with $\lambda = 1$, specifically $\bar{\mathbf{r}}_{d6} = [0 \ 0 \ 1 \ 0 \ 0 \ 1]^T$. This indicates that any geometry where the source and sensor are collocated at a point on the z axis is degenerate with respect to operations e and g_6 . Therefore, from (27) we can determine

$$\begin{aligned} \overset{\leftrightarrow}{\mathbf{G}}(\bar{\mathbf{r}}_{d6}, \bar{\mathbf{r}}'_{d6}) &= \begin{bmatrix} g_{xx}(\bar{\mathbf{r}}_{d6}, \bar{\mathbf{r}}'_{d6}) & g_{xy}(\bar{\mathbf{r}}_{d6}, \bar{\mathbf{r}}'_{d6}) & g_{xz}(\bar{\mathbf{r}}_{d6}, \bar{\mathbf{r}}'_{d6}) \\ g_{yx}(\bar{\mathbf{r}}_{d6}, \bar{\mathbf{r}}'_{d6}) & g_{yy}(\bar{\mathbf{r}}_{d6}, \bar{\mathbf{r}}'_{d6}) & g_{yz}(\bar{\mathbf{r}}_{d6}, \bar{\mathbf{r}}'_{d6}) \\ g_{zx}(\bar{\mathbf{r}}_{d6}, \bar{\mathbf{r}}'_{d6}) & g_{zy}(\bar{\mathbf{r}}_{d6}, \bar{\mathbf{r}}'_{d6}) & g_{zz}(\bar{\mathbf{r}}_{d6}, \bar{\mathbf{r}}'_{d6}) \end{bmatrix} \\ &= \begin{bmatrix} g_{yy}(\bar{\mathbf{r}}_{d6}, \bar{\mathbf{r}}'_{d6}) & -g_{xy}(\bar{\mathbf{r}}_{d6}, \bar{\mathbf{r}}'_{d6}) & -g_{zy}(\bar{\mathbf{r}}_{d6}, \bar{\mathbf{r}}'_{d6}) \\ -g_{yx}(\bar{\mathbf{r}}_{d6}, \bar{\mathbf{r}}'_{d6}) & g_{xx}(\bar{\mathbf{r}}_{d6}, \bar{\mathbf{r}}'_{d6}) & g_{zx}(\bar{\mathbf{r}}_{d6}, \bar{\mathbf{r}}'_{d6}) \\ -g_{yz}(\bar{\mathbf{r}}_{d6}, \bar{\mathbf{r}}'_{d6}) & -g_{xz}(\bar{\mathbf{r}}_{d6}, \bar{\mathbf{r}}'_{d6}) & g_{zz}(\bar{\mathbf{r}}_{d6}, \bar{\mathbf{r}}'_{d6}) \end{bmatrix} \quad (28) \end{aligned}$$

where position vectors $\bar{\mathbf{r}}_{d6}$ and $\bar{\mathbf{r}}'_{d6}$ both indicate the same point on the z axis (i.e., a degenerate geometry for $\overset{\leftrightarrow}{\mathbf{g}}_6$). Evaluating (28), it is evident that $g_{xx}(\bar{\mathbf{r}}_{d6}, \bar{\mathbf{r}}'_{d6}) = g_{yy}(\bar{\mathbf{r}}_{d6}, \bar{\mathbf{r}}'_{d6})$ and that all off-diagonal elements of $\overset{\leftrightarrow}{\mathbf{G}}(\bar{\mathbf{r}}_{d6}, \bar{\mathbf{r}}'_{d6})$ are zero.

Essentially, (27) provides the general polarimetric response of symmetric targets for the bistatic measurement geometries described by (26). Since the matrix representation of group \mathcal{C}_{4ar} consists of 16 elements $\overset{\leftrightarrow}{\mathbf{g}}_n$, (26) provides 16 sets of eigenvectors from which to construct degenerate geometries; and from (27), a general form of the scattering dyadic $\overset{\leftrightarrow}{\mathbf{G}}(\bar{\mathbf{r}}_{dn}, \bar{\mathbf{r}}'_{dn})$ can be determined for each of these 16 degenerate geometries. For many of the 16 solutions, the off-diagonal elements are zero,

thus providing an exact scattering solution for any object with \mathcal{C}_{4a} symmetry. These zero-valued solutions are analogous to the far-field backscattering case where it is well known that a BOR exhibits no cross-polarized response [22]. Equation (27), however, provides all zero-valued solutions for more general scattering cases (i.e., near-field, bistatic), as well as for more general target symmetries.

V. SUBSURFACE TARGET IDENTIFICATION

The results of Section IV demonstrate that scattering from symmetric targets exhibits a multitude of dependencies in terms of spatial location as well as polarization. From the standpoint of subsurface target classification, the appearance of these dependencies in bistatic measurements would suggest the presence of a symmetric target (i.e., a landmine), whereas the absence of these relationships would indicate a nonsymmetric target (e.g., subsurface clutter). A strength of this idea is that these spatial scattering dependencies are exhibited by all symmetric targets that possess the symmetry of a given group, regardless of target size, shape, or material. Additionally, for symmetric objects buried in a dielectric half-space (e.g., soil), these scattering dependencies are valid regardless of depth or properties of the surrounding soil. As a result, scattering features can be constructed from sets of bistatic measurements such that the symmetry of an observed target could be indicated. Moreover, these features can be constructed such that they are invariant to target size, shape, material, etc. This is in contrast to the temporal scattering response of targets, wherein no such invariant feature can be constructed.

Given the scattered field defined in (3), the complex measurement $v(t)$ of a bistatic radar can be described as

$$v(t) = \int_V \int_{-\infty}^t \bar{\mathbf{w}}(\bar{\mathbf{r}}; t, t') \cdot \bar{\mathbf{E}}(\bar{\mathbf{r}}, t') dV dt' \quad (29)$$

where $\bar{\mathbf{w}}(\bar{\mathbf{r}}; t, t')$ describes the spatial and temporal response of the receiver and its antenna, including any temporal signal processing. In general, the response $v(t)$ is dependent entirely on the radar and target parameters. However, for many of the degenerate bistatic geometries described in Section IV, the orientation of a receive vector $\bar{\mathbf{w}}$ and a source vector $\bar{\mathbf{J}}$ can be chosen such that the response from a symmetric target will be zero (i.e., $v(t) = 0$), regardless of other target or sensor parameters. Thus, a nonzero response from such a degenerate bistatic measurement, or set of measurements, would indicate a nonsymmetric target. The converse, of course, is not true. A zero-valued response from a set of degenerate measurements *may* indicate a symmetric target, but this null response would likewise be observed if no target were present. Therefore, in addition to zero-valued degenerate measurements, other scattering measurements are required to both detect and classify an object.

Measurements using nondegenerate bistatic geometries can likewise be used to evaluate target symmetry. Unlike degenerate geometries, where a single bistatic observation can indicate symmetry, pairs of nondegenerate measurements must be evaluated. As stated before, two bistatic measurements related by an operation g_n of a specific bistatic group will be identical if the target has the corresponding group symmetry—a result mathematically expressed by (22). Therefore, a symmetric

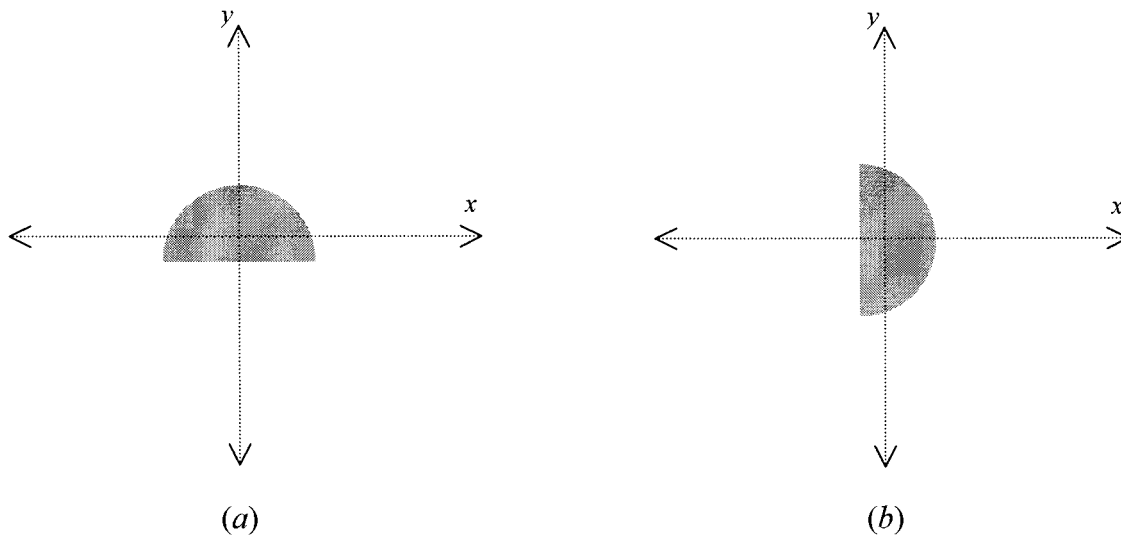


Fig. 5. Diagram of targets used in the symmetry detection experiment. Target (a) exhibits bilateral (i.e., reflection) symmetry with respect to the plane $x = 0$, while target (b) does not.

target would be indicated if the two related measurements produced identical responses, whereas dissimilar responses would indicate a nonsymmetric object. Although nondegenerate geometries require two bistatic measurements to evaluate target symmetry (as opposed to a single measurement for degenerate cases), this method has the advantage that each measurement will almost certainly be nonzero when a target is present. Thus, a pair of bistatic measurements, related by g_n , provides information useful for both target detection and classification.

Of course, when observing a symmetric target, a pair of related bistatic observations will never be *exactly* identical, nor will a degenerate measurement be exactly zero. Measurement error including noise, antenna asymmetry, measurement bias, and positioning error can corrupt the bistatic measurements. Additionally, the illuminated target may be imperfectly symmetric: surface roughness, soil inhomogeneity, or imperfect orientation of the object will perturb the measurement symmetry. Therefore, to provide a numeric value of the similarity between two bistatic measurements, the following measure has been proposed [23, pp. 992–1002]:

$$m(n) = \frac{\int |v_0(t) - v_n(t)|^2 dt}{\int |v_0(t) + v_n(t)|^2 dt} \quad (30)$$

where the bistatic geometry that produces $v_0(t)$ is related to that of $v_n(t)$ by group operation g_n . Note that this function produces a real, nonnegative coefficient that is zero valued when the two measurements are identical. The denominator of (30) is effectively a normalization factor, so that the expected value of $m(n)$ approaches 1.0 as measurement the signal-to-noise ratio (SNR) is reduced to zero. Accordingly, bistatic measurements of sufficient SNR will ideally produce a coefficient $m(n) \ll 1$ for any symmetric target, regardless of size, shape, depth, or material.

Again, the converse is not necessarily true: a single pair of bistatic observations of an asymmetric target may also produce nearly identical measurements and, therefore, a small value of $m(n)$. Ideally then, a large and diverse collection of measures

$m(n)$, formed from different bistatic geometries, would be implemented in order to make a target classification. For a symmetric target, all of the values $m(n)$ would be small, whereas an asymmetric target would produce some large values of $m(n)$ almost certainly. However, considerations such as cost and complexity limit the practical number of measurements and thus coefficients $m(n)$ that can be determined for a given target. A question then is, can symmetry be effectively used to classify subsurface targets? Given measurement error and the fact that asymmetric targets may appear symmetric, can we accurately discriminate between symmetric mines and asymmetric clutter, given a limited set of bistatic measurements?

To provide some insight into these questions, an extensive set of bistatic measurements, covering 2–6 GHz, was taken in the GPR test facility at the Radar Systems and Remote Sensing Laboratory (RSL) at the University of Kansas. More than 2000 bistatic measurements were made by positioning transmitter and receiver antennas at all possible locations on a 5.0-cm Cartesian lattice, extending over a surface area of 30.0 cm \times 30.0 cm. These measurements were taken on a target that possessed reflection symmetry across the $x = 0$ plane (i.e., group \mathcal{R}), as well as on another that did not possess this symmetry. Each bistatic measurement was paired with its reflection across the $x = 0$ plane, i.e., the bistatic pairs were related by the operation $g_n = \sigma_a$. Each bistatic measurement was processed by subtracting the average specular surface response and then time gating such that the surface response was removed. A coefficient denoted $m(\sigma_a)$ was then calculated for each bistatic pair, with the exception of cases where the bistatic pairs were, likewise, related by the transpose operation π . For these degenerate geometries, reciprocity would ensure that the symmetry coefficient $m(\sigma_a)$ would equal zero, regardless of the symmetry of the target.

The same object was employed as both the symmetric and asymmetric target. A metal half-disk, 2.5-cm thick and with a radius of 8.0 cm, was used as the subsurface scatterer. The object was oriented so that its plane of reflection symmetry was either parallel with the $x = 0$ plane, producing a symmetric

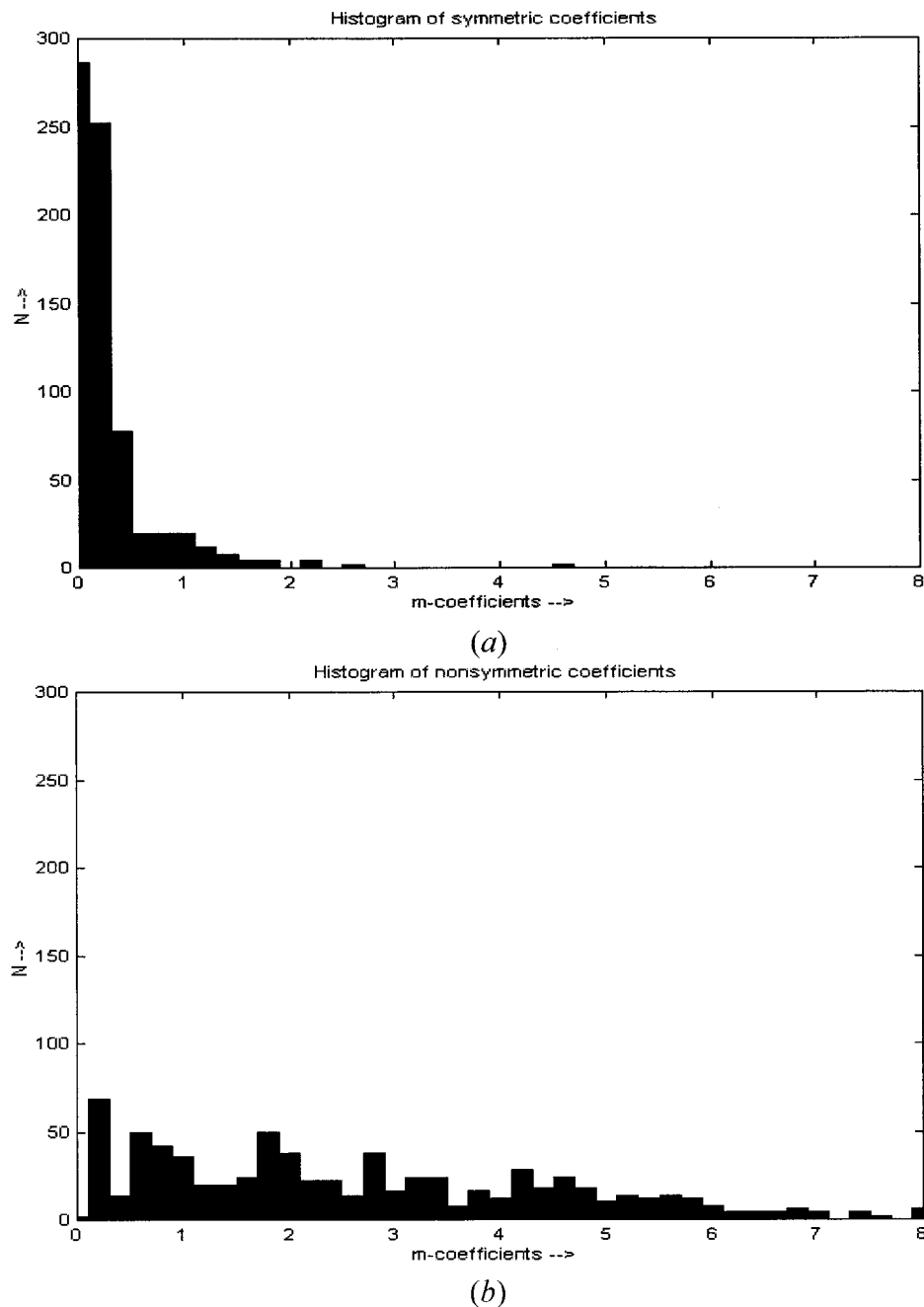


Fig. 6. Histogram of $m(\sigma_a)$ coefficient values calculated from a set of 2000 bistatic measurements. For a symmetric target (a), most values were much less than one, whereas the asymmetric target (b) produced values over a wide range.

target with respect to the measurements, or perpendicular to the $x = 0$ plane, producing an asymmetric target with respect to the measurements (see Fig. 5). This method was chosen in order to provide a controlled experiment; with the exception of their orientation, the two targets are identical in every respect. The differences in the two sets of bistatic data can, therefore, be attributed completely to differences in their reflection symmetry across the plane $x = 0$.

The bistatic measurements were used to calculate more than 700 different values of $m(\sigma_a)$ for both the symmetric and asymmetric targets. The results are presented in Fig. 6 in histogram form. It is apparent that for the symmetric target, nearly all values are much less than one (i.e., $m(\sigma_a) \ll 1$). The few

large values of $m(\sigma_a)$ result from bistatic measurements with poor SNR. Conversely, the values $m(\sigma_a)$ resulting from asymmetric target measurements are distributed across a wide range of values, from nearly zero to greater than 8.0. The results are as expected. The values for the symmetric target are small but not exactly zero, a result of normal measurement error. Additionally, the target was not oriented nor aligned with any precision other than that provided by the human eye, and no effort was made to flatten the sand surface. With regard to the asymmetric target, we note that a significant portion of the values $m(\sigma_a)$ are much less than one.

Thus, these data verify that a symmetric target will nearly *always* appear symmetric ($m(\sigma_a) \ll 1$), whereas an asymmetric

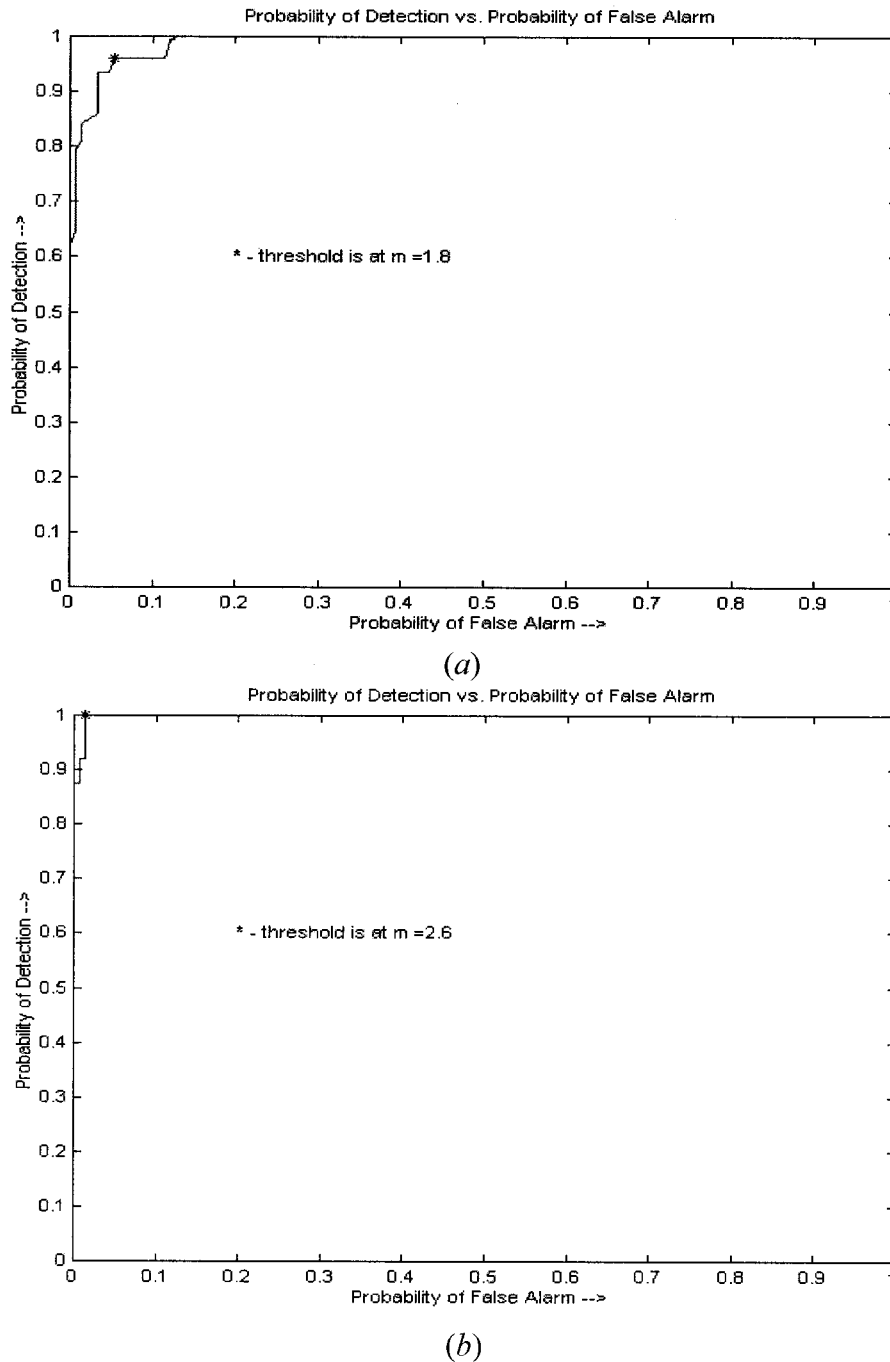


Fig. 7. Results of Monte Carlo symmetry detection test, presented as ROC. Random collections of three mirrored bistatic measurements were used for curve (a), while curve (b) shows the results when random collections of five bistatic measurements were used.

target will *often* appear asymmetric. Given this ambiguity, a question remains as to the efficacy of target classification based on the symmetry measure $m(\sigma_a)$. To provide an answer, at least for this specific experiment, a target detection evaluation was performed using Monte Carlo analysis. To begin the analysis, a small collection of bistatic pairs (related by σ_a) was randomly selected from the overall set of bistatic measurements for each target. The symmetry measure $m(\sigma_a)$ from a given bistatic pair was then compared to a threshold γ . If $m(\sigma_a) < \gamma$, the target was classified as symmetric; otherwise it was classified as asymmetric. This comparison was repeated for each bistatic pair of the small measurement collection, and then a final dec-

laration was made using a "unanimous voting rule" approach, wherein the target was declared symmetric only if *every* measurement indicated target symmetry (i.e., no $m(\sigma_a) > \gamma$ in the collection). If measurements of the symmetric target were used, and the target was correctly declared symmetric, a detection was recorded. Alternatively, a false alarm was recorded if measurements of the asymmetric target were used and if the target was incorrectly identified as symmetric. A new collection of bistatic measurements was then randomly selected from the overall measurement set, and the above procedure was repeated. After this procedure was performed on a large number of random collections, a probability of detection was determined

as the percentage of declared symmetric target detections, while the probability of false alarm was similarly determined from the number of false alarms. The entire Monte Carlo procedure was, likewise, repeated using different values of threshold γ , from $\gamma = 0$ to a large value where the probability of false alarm became equal to one.

The results of this Monte Carlo analysis are presented as a receiver operating curve (ROC) in Fig. 7. Curves for classification using collections of three bistatic pairs and seven bistatic pairs are presented, and they show that for this particular measurement set, nearly perfect classification can be achieved using as few as three values of $m(\sigma_a)$. This experiment does not prove or otherwise provide a specific numerical determination of the general efficacy of symmetry features for classifying subsurface targets, particularly with respect to discriminating between landmines and clutter objects. The problem is, of course, very scenario dependent, and results will be a function of the subsurface environment, sensor parameters, and the specific targets involved. Nevertheless, these experimental results do suggest that bistatic symmetry measures can likely provide useful information for target classification—information that does not require training data nor any other *a priori* knowledge about mine targets.

However, it should be stated that several problems could potentially reduce the efficacy of symmetry-based detection. Foremost among these is the problem of clutter targets located in proximity to a mine. This occurrence could destroy scattering symmetry and potentially result in poor detection performance. Ultimately, this problem is dependent on sensor resolution: the GPR must be able to separate the mine response from surrounding clutter, including the surface. A GPR suitable for mine symmetry detection would require sufficient aperture size and bandwidth to provide subsurface resolution on the order of the physical dimensions of a mine. As a result, the mine would likely be the dominant scatterer within a resolution cell, and the scattering associated with that cell would appear symmetric. For example, work is currently being conducted using GPR bistatic antenna arrays to provide spatial resolution, as well as symmetry evaluation for every subsurface resolution cell.

Of course, the subsurface clutter environment can become so severe that symmetry detection will be defeated, regardless of sensor symmetry or processing. This, however, is arguably true for all feature-based detection techniques. The relevant question is how robust a technique is when encountering subsurface clutter. It is important to note that the technique described in this section does not require perfect scattering symmetry, as this cannot be achieved. Rather, the symmetry coefficients $m(n)$ provide a continuous measure of the *degree* of apparent symmetry: small values indicate high symmetry, while large values indicate low symmetry. As Figs. 6 and 7 suggest, a mine can be distinguished in a clutter environment if the mine appears significantly *more* symmetric than the surrounding clutter objects (e.g., rocks). In other words, the appearance of *perfect* target symmetry is not a requirement to perform target discrimination based on symmetry. With sufficient sensor resolution and a significant collection of symmetry measures $m(n)$, a mine residing in a clutter environment would likely appear more symmetric than rocks residing in that same environment.

Another obvious problem is that for demining applications, the location of the target is not known. How can symmetric bistatic measurements be constructed, if the location of a symmetric plane or axis of rotation is unknown? A symmetric sensor must first be constructed and then scanned across a test area. At each location, a hypothesis is tested: is there a target here, and does it appear to be symmetric? When the sensor symmetry aligns with the target's, the answer should be affirmative. This approach is consistent with mine detection equipment; either hand-held or vehicle-mounted, the sensor moves across a given area, testing the mine hypothesis at every location.

VI. CONCLUSIONS

Group theory provides a mathematical tool for analyzing physical problems where symmetries exist. An example of such a problem is the electromagnetic scattering from landmines, which typically exhibit geometric symmetry. In this paper, we have demonstrated how group-theoretic techniques can be used to identify the general form of the dyadic Green's function of a symmetric scatterer, including all dependent relationships of position and polarization. Likewise, it was shown that group-theoretic techniques can be used to determine all zero-valued scattering responses of a symmetric target, responses that are independent of other target parameters. Although the analysis focused on scattering from targets possessing \mathcal{C}_{4a} symmetry (typical of mines), the results could also be applied to targets with dihedral or rotation-reflection symmetry, as well as regular polyhedra.

This group-theoretic analysis showed that a symmetric target produces a scattering response with a surprising number of dependencies in terms of position and polarization. These dependencies provide a mechanism for evaluating the symmetry of an unknown target, a mechanism that is otherwise independent of target parameters. Laboratory tests indicate that these symmetric scattering responses are sufficiently powerful to facilitate target classification, given the presence of normal measurement error.

Of course, as with other approaches, conditions can occur that will defeat symmetry detection, such as severe clutter, low SNR, asymmetric mines, or symmetric clutter objects. However, symmetry feature detection is perhaps unique in that it provides a detection method that does not require training data or specific scattering formulations. Further, it is independent of soil moisture or target depth. Thus, a detector can potentially be constructed that is independent of specific mine type or soil condition.

REFERENCES

- [1] L. P. Peters, J. J. Daniels, and J. D. Young, "Ground-penetrating radar as a subsurface environmental sensing tool," *Proc. IEEE*, vol. 82, pp. 1802–1822, Dec. 1994.
- [2] T. P. Montoya and G. S. Smith, "Landmine detection using a ground-penetrating radar based on loaded vee dipoles," *IEEE Trans. Antennas Propagat.*, vol. 47, pp. 1795–1806, Dec. 1999.
- [3] P. D. Gader, B. Nelson, H. Frigui, G. Vailllette, and J. Keller, "Landmine detection in ground-penetrating radar using fuzzy logic," *Fuzzy Logic Signal Process.*, vol. 80, pp. 1069–1084, June 2000.
- [4] P. D. Gader, M. Mystkowski, and Y. Zhao, "Landmine detection with ground-penetrating radar using hidden Markov models," *IEEE Trans. Geosci. Remote Sensing*, vol. 39, pp. 1231–1244, June 2001.

- [5] S. Vitebskiy and L. Carin, "Resonances of perfectly conducting wires and bodies of revolution buried in a lossy, dispersive half-space," *IEEE Trans. Antennas Propagat.*, vol. 28, pp. 1575–1583, Dec. 1996.
- [6] N. Geng, D. R. Jackson, and L. Carin, "On the resonances of a dielectric BOR buried in dispersive layered medium," *IEEE Trans. Antennas Propagat.*, vol. 47, pp. 1305–1313, Aug. 1999.
- [7] T. Dogaru, L. Collins, and L. Carin, "Optimal time-domain detection of a deterministic target buried under a randomly rough interface," *IEEE Trans. Antennas Propagat.*, vol. 49, pp. 313–326, Mar. 2001.
- [8] H. Weyl, *Symmetry*. Princeton, N.J.: Princeton Univ. Press, 1952.
- [9] R. McWeeny, *Symmetry: An Introduction to Group Theory and Its Applications*. New York: MacMillan, 1963.
- [10] M. Hamermesh, *Group Theory and Its Application to Physical Problems*. New York: Dover, 1989.
- [11] B. Lahme and R. Miranda, "Karhunen-Love decomposition in the presence of symmetry," *IEEE Trans. Image Processing*, vol. 8, pp. 1183–1190, Sept. 1999.
- [12] C. E. Baum and H. N. Kritikos, Eds., *Electromagnetic Symmetry*. New York: Taylor & Francis, 1995.
- [13] V. A. Dmitriyev, "Symmetry of microwave devices with gyrotropic media-complete solution and applications," *IEEE Trans. Microwave Theory Tech.*, vol. 45, pp. 394–401, Mar. 1997.
- [14] N. Kishi, K. Tayama, and E. Yamashita, "Modal analysis of optical fibers with symmetrically distributed nonuniform cores," *J. Lightwave Technol.*, vol. 14, pp. 1794–1800, Aug. 1996.
- [15] C. E. Baum, "Symmetry in electromagnetic scattering as a target discriminant," U.S. Air Force Res. Lab. Interaction Note 523, Oct. 1996.
- [16] H. Kritikos, "Rotational symmetries of electromagnetic radiation fields," *IEEE Trans. Antennas Propagat.*, vol. 31, pp. 377–382, Mar. 1983.
- [17] —, "Group symmetries of antenna arrays," in *Recent Advances in Electromagnetism*, H. Kritikos and D. Jaggard, Eds. New York: Springer-Verlag, 1990.
- [18] A. V. Shubnikov and V. A. Koptsik, *Symmetry in Science and Art*. New York: Plenum, 1974.
- [19] H. Weyl, *The Classical Groups*. Princeton, N.J.: Princeton Univ. Press, 1939.
- [20] W. Magnus, A. Karrass, and D. Solitar, *Combinatorial Group Theory: Presentations of Groups in Terms of Generators and Relations*. New York: Dover, 1976.
- [21] C. Tai, *Dyadic Green Functions in Electromagnetic Theory*. Piscataway, NJ: IEEE Press, 1994.
- [22] L. Carin, N. Geng, M. McClure, J. Sichina, and L. Nguyen, "Ultra-wide-band synthetic aperture radar for minefield detection," *IEEE Antennas Propagat. Mag.*, vol. 41, pp. 18–33, Feb. 1999.

- [23] J. M. Stiles, P. Parra-Bocaranda, and A. Apte, "Detection of object symmetry using bistatic and polarimetric GPR observations," *Proc. SPIE*, vol. 3710, Apr. 1999.

James M. Stiles (S'91–M'95–SM'97) received the B.S. degree in electrical engineering from the University of Missouri, Columbia, in 1983, the M.S. degree in electrical engineering from Southern Methodist University, Dallas, TX, in 1987, and the Ph.D. degree in electrical engineering from the University of Michigan, Ann Arbor, in 1996.

He is currently an Associate Professor in the Department of Electrical Engineering and Computer Science at the University of Kansas, Lawrence, and a Member of the Radar Systems and Remote Sensing Laboratory (RSL). He has been with the University of Kansas since 1996. From 1983 to 1990, he was a Microwave Systems Design Engineer for Texas Instruments, and from 1990 to 1996, he was a Graduate Research Assistant in the Radiation Laboratory at the University of Michigan. His research interests include radar remote sensing of vegetation, propagation and scattering in random media, ground-penetrating radar, and radar signal processing.

Abhijit V. Apte received the B.S. degree in electronics and telecommunication from the University of Bombay, Bombay, India, and the M.S. degree in electrical engineering from the University of Kansas, Lawrence.

Since August 2000, he is currently with Sprint's Broadband Wireless Group as an RF Engineer. From 1998 to 2000, he was a Research Assistant in the project on the landmine detection using ground-penetrating radar, at the Radar Systems and Remote Sensing Laboratory (RSL), University of Kansas. His research was related to the detection of landmines using the symmetry property of man-made objects and using the symmetry property to separate landmines from the surrounding clutter.

Beng Beh received the B.S. and M.S. degrees in electrical engineering from the University of Kansas, Lawrence, in 1992 and 1997, respectively.

Currently, he is a Test Engineer with Winbond Electronic Corporation America, San Jose, CA. He was an Electronic Test Engineer with Hewlett-Packard Malaysia from 1992 to 1994. From 1995 to 2001, he was a Graduate Research Assistant with the Radar System and Remote Sensing Laboratory at the University of Kansas.